ELSEVIER

Thermochimica Acta 360 (2000) 157–168

thermochimica acta

www.elsevier.com/locate/tca

Some elements in specific heat capacity measurement and numerical simulation of temperature modulated DSC (TMDSC) with *R*/*C* network

S.X. Xu[a,*], Y. Li[a], Y.P. Feng[b]

[a]*Department of Materials Science, National University of Singapore, Faculty of Science, Lower Kent Ridge Road, Singapore, Singapore*
[b]*Department of Physics, National University of Singapore, Faculty of Science, Lower Kent Ridge Road, Singapore, Singapore*

Received 14 March 2000; accepted 6 June 2000

Abstract

One important application of temperature modulated DSC (TMDSC) is the measurement of specific heat of materials. In this paper, a thermal resistance/capacitance (*R*/*C*) numerical model is used to analyze the effects of experimental parameters and calibration on the measurement of specific heat in TMDSC under isothermal conditions. The actual TMDSC experiments were conducted with sapphire and pure copper samples, respectively. Both simulation and experiments showed that in TMDSC, the measured sample specific heat is a non-linear function of many factors such as sample mass, the heat transfer properties of the TMDSC instrument, temperature modulation period, the heat capacity difference between calibration material and the test material, but modulation amplitude has very little effect on the results. The typical behavior of a heat flux type TMDSC can be described as a low pass filter in terms of specific heat capacity measurement when the instrument heat transfer properties are taken into account. At least for metallic materials, where the temperature gradient inside the sample can normally be ignored, the sample should be chosen in such a way that its total heat capacity (mass times specific heat) is close to that of the calibration material in order to get a more accurate result. Also, a large modulation period is beneficial to improving the test accuracy.

Keywords: TMDSC; Specific heat capacity; Heat capacity

1. Introduction

Temperature modulated differential scanning calorimetry (TMDSC), which was first introduced by Reading et al. [1] in 1992, became commercialized shortly afterwards and is being widely applied to materials research including polymeric, food, pharmaceutical and metallic materials. TMDSC, where normally a sinusoidal temperature change is superimposed onto a linear underlying heating rate, can be used to measure materials thermal properties such as specific heat. Specific heat measurement under isothermal conditions (the underlying heating rate is zero) with TMDSC was also reported [2–3].

Although both conventional DSC and TMDSC are used for specific heat measurement, their experimental and mathematical methods are quite different.

In an ideal heat flux type differential scanning calorimetry system, where the instrument thermal inertial, the heat exchange between the heating block and the sample by purge gas convection and thermal radiation can be ignored, and also if there is no kinetic event and temperature gradient inside the sample, it

* Corresponding author.
E-mail address: scip7317@nus.edu.sg (S.X. Xu).

0040-6031/00/$ – see front matter
PII: S0040-6031(00)00566-9

can be shown that sample heat capacity can be obtained by Wunderlich et al. [3].

$$C'_s = \frac{A_{\Delta T}}{A_{Ts}} \sqrt{\left(\frac{K}{\omega}\right)^2 + C_r^2} = \frac{A_{\Delta T} K}{A_{Ts}\omega} \sqrt{1 + \left(\frac{\omega C_r}{K}\right)^2} \quad (1)$$

where C'_s is the sample's heat capacity, $A_{\Delta T}$ the reference-sample temperature difference amplitude, C_r the heat capacity of the reference, K the system thermal constant, A_{Ts} the sample temperature amplitude and ω the temperature modulation angular frequency.

In the case of TMDSC instrument, the apparent or measured sample heat capacity C'_{s_m} is obtained by,

$$C'_{s\_m} = \frac{KA_{\Delta T}}{A_{Ts}\omega} \quad (2)$$

In the above equation, $KA_{\Delta T}$ equals the amplitude of modulated heat flow. The difference between Eqs. (1) and (2) is that in Eq. (1), there is a TMDSC test system related item $\sqrt{1 + (\omega C_r/K)^2}$, which can be obtained by a calibration material with a known heat capacity, for example, sapphire sample. And this calibration factor K_{C_p} can then be used to modify the apparent sample heat capacity C'_{s_m}. That is, C'_s should equal $K_{C_p} C'_{s\_m}$. By dividing this value with the sample's mass M_s, we obtain its specific heat capacity as $C_p = K_{C_p} C'_{s\_m}/M_s$.

For such an oversimplified TMDSC model, according to Eqs. (1) and (2), the measured sample specific heat should not be sample mass dependent. So long as the values for system constant K, C_r, ω, $A_{\Delta T}$ and A_{Ts} are accurate, the heat capacity and hence the specific heat of the sample can be accurately obtained. But experiments showed that the measured sample specific heat capacity is not only mass dependent but also dependent on the modulation frequency even if the measured value has been corrected with the calibration factor K_{C_p} obtained from a standard material with a known C_p under exactly the same modulation conditions (e.g. same modulation amplitude and frequency, et al.). These deviations could be partly attributed to the thermal gradient that is built up inside the sample [2,4–6]. Merzlyakov and Schick [7] investigated the theoretical aspect of power compensation DSC, finding that apparent heat capacity systematically drops with different temperature sensing positions and also that the calibration factor is a very complicated function of the sample itself. Our study shows that heat transfer properties in a heat flux TMDSC instrument such as the thermal resistance between the thermal couple and sample or reference also play important roles.

In this paper, a thermal resistance/capacitance network model was adopted to study the effect of TMDSC instrument properties and experimental parameters in C_p test.

2. Modeling and experiments

To explain the above mentioned effects of sample mass, modulation period, etc., other factors such as the instrument itself has been taken into account in the model. Under all conditions it is assumed that thermal gradient inside the sample is negligible. First, we may take a look at the melting process of indium sample in conventional DSC.

2.1. Indium melting experiment in conventional DSC

Fig. 1 shows the heat flow and the sample temperature curves as a function of time for a pure indium sample with a mass of 15.50 mg at a heating rate of 10 K/min in conventional DSC. In the sample temperature curve, point A is the melting onset point and B is the melting ending point. After point B, the sample temperature quickly catches up with the programmed temperature. Due to the extremely narrow melting temperature region of pure indium, when the sample begins to melt, its real temperature should be fairly constant, which should generate a flat platform in the temperature curve during melting.

In a typical heat flux type DSC/TMDSC cell (see Fig. 2), the temperature sensors are located somewhat below the sample and reference pan. The tested temperature is not the sample's exact temperature but the temperature of the point where the sensor is positioned. Thus, it can be seen that between points A and B, this temperature is still rising in the melting event (Fig. 1).

Fig. 3 shows that the temperature rising rates of the sample sensor in the region of melting between points A and B are quite significant under various heating rates (from 1 to 40 K/min). There is a remarkable linear relationship between these two rates: the sample sensor temperature slope is ca. 70% of the

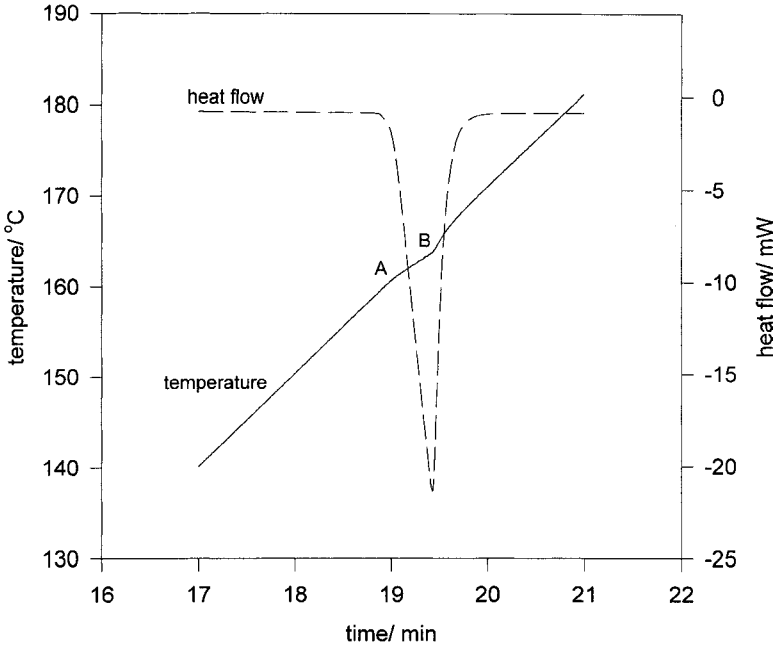

Fig. 1. An indium melting curve in conventional DSC, sample size is 15.50 mg.

programmed heating rate during the melting between points A and B. From this result, it is reasonable to conclude that considerable thermal resistance exists between the temperature sensor and the sample itself.

2.2. System thermal constant K

The instrument system thermal constant K is obtained by analyzing the heat flow signal, the corresponding $\Delta T(=T_r-T_s)$ which is actually given in micro volt, and the thermal couple's thermal-electric properties. K is found to be ca. 0.01 W/K for TA Instruments DSC2920 cell, which translates into an overall 100 K/W cell thermal resistance.

When the thermal resistance and the heat capacities of the TMDSC cell itself are included, the model represented by an equivalent resistor/capacitor (R/C) network is given as shown in Fig. 4,

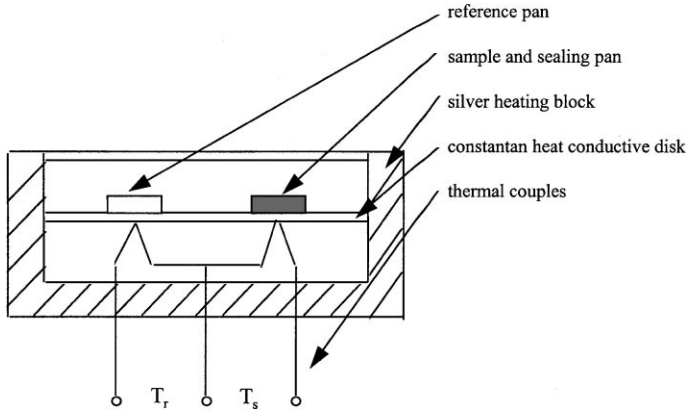

Fig. 2. A simplified TMDSC cell structure.

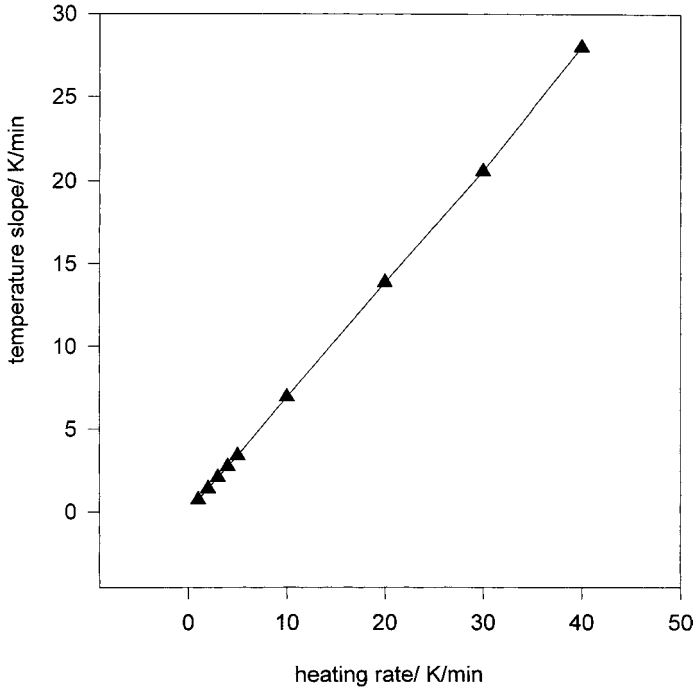

Fig. 3. Sample thermal couple temperature slope between points A and B (see Fig. 1) as a function of DSC heating rate, demonstrating a good linear relationship between them.

R_1 to R_4 are the thermal resistances of the heat conducting path, the constantan disk,
R_r and R_s are the thermal resistances between the thermal couples and the reference or sample, respectively,
C_1 to C_4 are the heat capacities of the heat transfer path, respectively,
T_r is the reference side thermal couple temperature,
T_{r1} is the reference's real temperature,
T_s is the sample side thermal couple temperature,
T_{s1} is the sample's true temperature.

Hence, we can obtain the following thermal conducting equations,

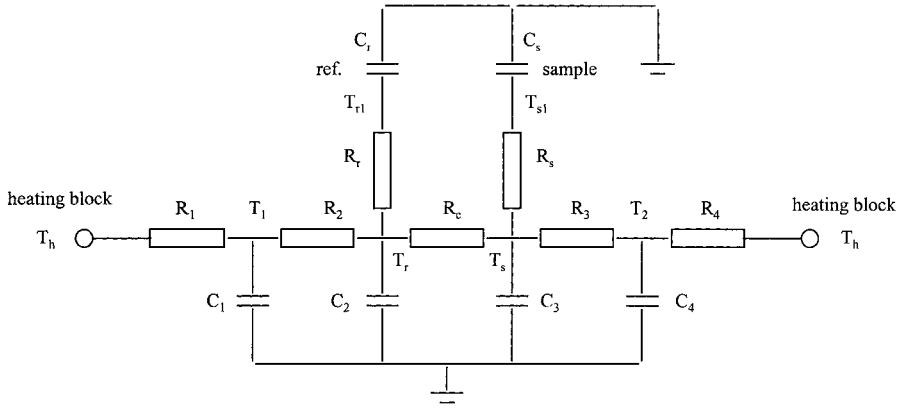

Fig. 4. TMDSC model represented with thermal resistance and capacitance (R/C) network.

$$\frac{T_h - T_1}{R_1} = \frac{T_1 - T_r}{R_2} + C_1\left(\frac{dT_1}{dt}\right) \quad (3)$$

$$\frac{T_h - T_2}{R_4} = \frac{T_2 - T_s}{R_3} + C_4\left(\frac{dT_2}{dt}\right) \quad (4)$$

$$\frac{T_1 - T_r}{R_2} = \frac{T_r - T_s}{R_c} + \frac{T_r - T_{r1}}{R_r} + C_2\left(\frac{dT_r}{dt}\right) \quad (5)$$

$$\frac{T_2 - T_s}{R_3} = \frac{T_s - T_r}{R_c} + \frac{T_s - T_{s1}}{R_s} + C_3\left(\frac{dT_s}{dt}\right) \quad (6)$$

$$\frac{T_r - T_{r1}}{R_r} = C_r\left(\frac{dT_{r1}}{dt}\right) \quad (7)$$

$$\frac{T_s - T_{s1}}{R_s} = C_s\left(\frac{dT_{s1}}{dt}\right) \quad (8)$$

Finite difference method is used to solve the heating equations involved in this model, with a small time step of 0.0001 s. The parameters used in the simulation are listed in Table 1. A perfectly symmetric TMDSC cell was assumed. Because it is difficult to obtain the actual heat transfer parameters of the cell, for the sake of simplicity, we further assume $R_1=R_2=R_3=R_4$, $R_r=R_s$, $C_1=C_2=C_3=C_4$.

2.3. Isothermal TMDSC experimental conditions

A standard sapphire disk supplied by TA Instruments with a mass of 18.25 was used for TMDSC experiments as the calibration sample, the disk was sealed in an aluminum pan. Another five pure copper (>99.99%) samples with mass between 4.45 and 65.61 mg were used as the test material in later TMDSC runs. These copper samples were flattened and also sealed in aluminum pans to ensure good contact. The copper is chosen because of its very good thermal conductivity (thus to reduce the effect of temperature distribution unevenness as much as possible) and chemical stability in the temperature range studied as well as its well-known specific heat.

Isothermal TMDSC tests were conducted at 400 K with a modulation amplitude of 1 K and modulation periods of 30–100 s. Sample pans were carefully chosen so that they match the aluminum reference pan within a difference of 0.1 mg. The experiments were implemented on a TA Instruments DSC2920 system equipped with a rapid cooling system (RCS) which has a working temperature modulation period range between 10 and 100 s. And pure argon was used as the cell purge gas.

Table 1
TMDSC computer simulation parameters

Parameters	Description	Value
R_1–R_4	Thermal resistance of heat conducting path (K/W)	40
R_s, R_r	Thermal resistance between thermal couple and pan (in K/W)	70
C_1–C_4	Heat capacities of the heat conducting path (J/K)	0.01
T_0	Isothermal temperature (K)	400
A	Modulation amplitude (K)	1
dt	Time step for finite difference calculations (s)	0.0001
Period	Temperature modulation period (s)	30–100
C_r	Aluminum reference heat capacity (mJ/k)	22.824

3. Results and discussion

Fig. 5 shows the computer simulated 'real' sample/reference temperature T_{s1}, T_{r1} and 'measured' sample/reference temperatures T_s, T_r. Enough time was given for the system to reach a quasi-steady state without the effect of transient terms. As can be seen, there exist differences both in the amplitude and phase angle between the observed and real signals. Therefore, it is easy to image that the measured sample heat capacity will deviate from its original value.

3.1. Sample mass effect

The results of specific heat capacities of copper measured with different sample masses under various modulation periods by computer simulation and by experiment are plotted in Figs. 6 and 7, respectively. For each modulation period, a calibration factor was obtained with the 18.25 mg sapphire disk. (In the computer simulation, 'calibration factors' were determined by a virtual run of the sapphire, while in the experiments they were obtained by physically finding the ratio between the true specific heat and the measured sapphire specific heat). These calibration factors were then used in the copper samples TMDSC runs under the same modulation conditions to correct their specific heat. It is noticed that in Fig. 6, which shows the computer simulation results, a small sample mass

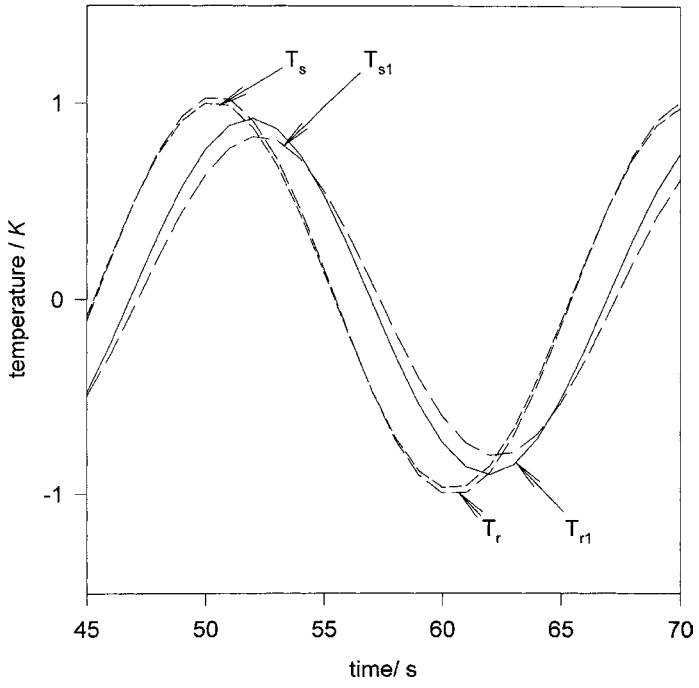

Fig. 5. Simulated 'real' sample/reference temperatures T_{s1}, T_{r1} vs. 'measured' sample/reference temperatures T_s, T_r (the thermal couple temperatures). Simulation conditions: M_s=20 mg, modulation period=20 s.

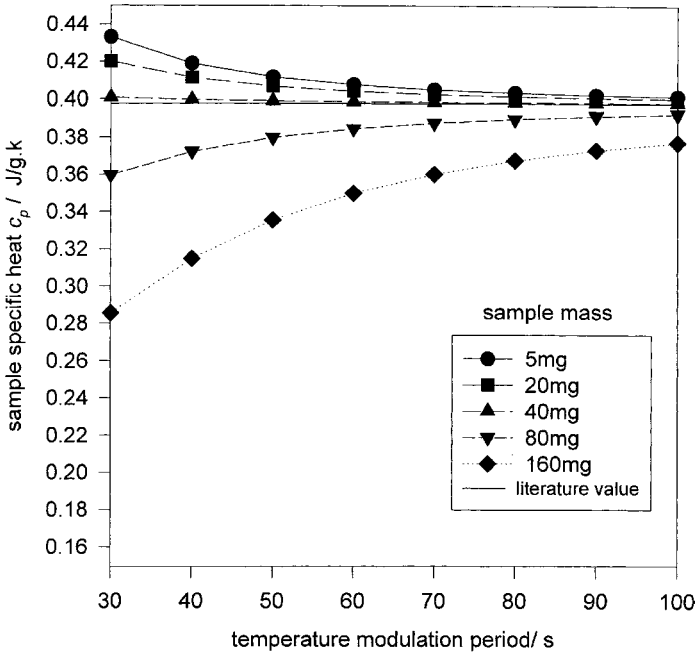

Fig. 6. Simulated copper sample mass and modulation period effect on the measured specific heat, which is obtained by using thermal couple temperatures T_r and T_s per Eqs. (1) and (2). (calibration factors K_{C_p} have been taken into account).

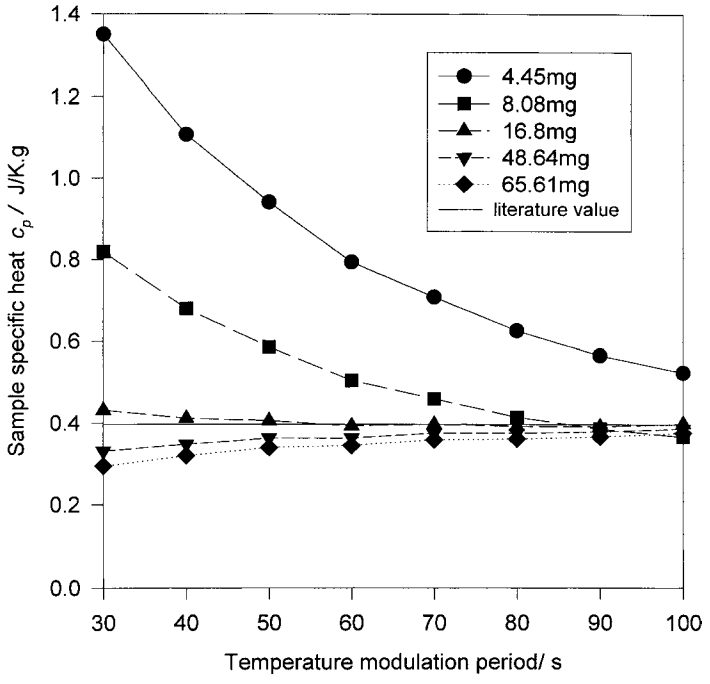

Fig. 7. Copper sample mass and modulation period effect on the measured specific heat (calibration factors K_{C_p} have been taken into account) by experiments conducted with a TA2920 system.

does not necessarily mean more accurate test results. If it is too small, as are the cases with the 5 and 20 mg copper samples, the specific heat capacity of copper by simulation will be higher than its literature value, which is 0.3975 J/g K for copper at 400 K [8]. Apparently the specific heat curve of the 40 mg sample shows the most stable results over the whole modulation frequencies, which exhibits only slight downward trend as the period increases. If the sample mass is too big, the 'measured' C_p values by simulation will be smaller than its real value, as are the cases for the 'samples' with a mass of 80 and 160 mg correspondingly.

Fig. 7 shows the specific capacity heat of copper obtained by experiments conducted with TA DSC2920. Samples with a mass of 4.45 and 8.08 mg exhibit a downward trend as the modulation period increases. The 16.8 mg curve drops slightly with period, while the rest of the samples exhibit an increasing trend with increasing period. There are other factors in the experiments which can make the results more complicated than those of the simulation, such as errors caused by TMDSC cell bias and purge gas convection which are not taken into consideration in the simulation. For example, the 8.08 mg sample data overlaps with that of the 65.61 mg sample when modulation period reaches 100 s. However, the general curve trends are still close to that of the simulation (Fig. 6), in that measured sample specific heat values by TMDSC are indeed mass sensitive. The sample mass should not be too small, which will cause higher than real specific heat values, nor should the mass be too large, which will end up with the values of tested C_p far below that of the real values even after calibration factors are taken into account.

Between the smaller mass samples that have a higher than its real C_p values and the larger mass samples with a lower than the real C_p values, there seems to be an optimal mass in which the sapphire calibration factor can almost completely give the measured C_p of test samples its true value. Results of simulation indicate that only when the total heat capacity of the test sample C'_s, which is the product of sample mass and its specific heat, equals that of calibration sample, the C_p of the test sample obtained will be the same as the true value independent of the

modulation period. Because in the model (see Fig. 4), the thermal couples can only 'feel' the sample's overall heat capacity, so long as they are the same for the calibration sample and the test sample, the measured temperature should be the same. If their overall heat capacities are different, then the calibration factor K_{C_p} obtained from the standard sapphire can not completely compensate the errors involved in the test sample. To be more specific, if the test sample's total heat capacity is lower than the sapphire disk's, the measured C_p will be higher than its real value, otherwise, it will be lower than the real specific heat. This deviation depends largely on the thermal properties of the test instrument, such as the thermal resistance and heat capacities of all the heat conducting paths. In the computer simulation, the total heat capacities of the five copper samples with a mass of 5, 20, 40, 80, and 160 are 0.002, 0.00795, 0.0159, 0.0318, 0.0636 J/K, respectively. The total heat capacity of the 18.25 mg sapphire calibration sample is: 0.0172 J/K, (sapphire specific heat=0.9423 J/g K at 400 K [9]), which is closest to the 40 mg copper sample's total heat capacity: 0.0159 J/K among the five values listed above, hence the best result is for the sample with a mass of 40 mg.

Experimental results agree with that of simulation. From Fig. 7, it can be seen that the optimal copper sample mass should be somewhere between 16.8 and 48.34 mg in order to obtain the most consistent specific heat capacity curve, which is least modulation period dependent.

3.2. TMDSC system output characteristics

Through TMDSC system output characteristics analysis, we can get a clearer picture on the above discussed non-linear effect. If we use the modulation frequency as the input, the ratio between measured sample heat capacity and sample real heat capacity $C'_{s\_m}/C'_s = 1/K_{C_p}$ as the output, the relationship between them is shown in Fig. 8, as can be seen clearly, sample with different total heat capacities follow different output curves. The bigger the total sample heat capacity C'_s, the lower the characteristic curve. These curves remind one of a typical low pass filter in a 'thermal version'. Now suppose the calibration

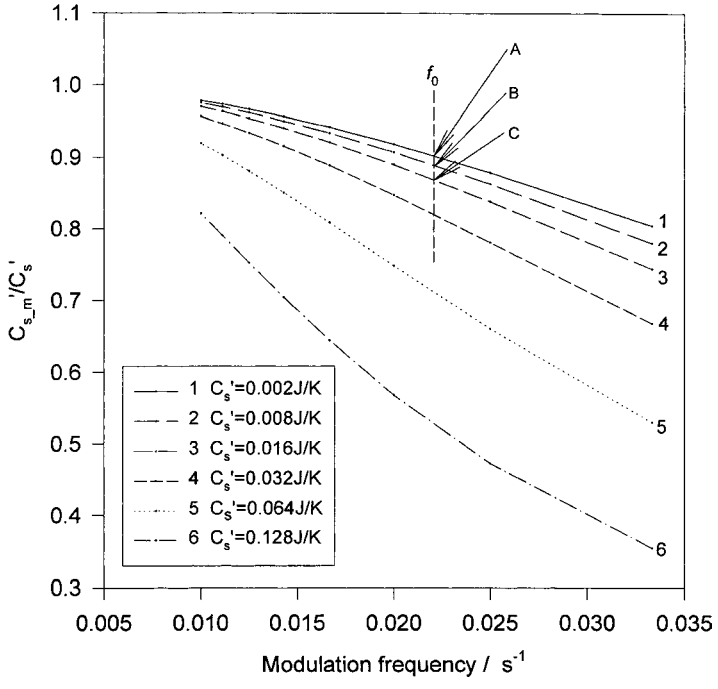

Fig. 8. Simulated TMDSC instrument output characteristics as a function of modulation frequency and the sample's total heat capacity.

sample has a heat capacity $C_{s\_calibration}$=0.008 J/K, its output curve will follow curve 2. At a given modulation frequency for example f_0, its C'_{s_m}/C_s value is at point B. The calibration factor can be denoted as $K_{C_p\_B}$. Then there are three possible situations for another sample to be tested.

1. $C'_s < C_{s\_calibration}$, for example, C'_s=0.002 J/K, hence it will follow curve 1, the accurate calibration factor it needs should be $K_{C_p\_A}$. Apparently, $K_{C_p\_B} > K_{C_p\_A}$, if $K_{C_p\_B}$ is used to correct the measured sample specific heat capacity, the result will be higher than its real value.
2. $C'_s = C_{s\_calibration}$, that is, C'_s=0.008 J/K, it will also follow curve 2, the accurate calibration factor it needs is the same: $K_{C_p\_B}$. Thus, the calibration factor obtained from the calibration sample can accurately correct the measured one for the test sample.
3. $C'_s > C_{s\_calibration}$, say, C'_s=0.016 J/K, it will then follow curve 3, the accurate calibration factor it needs should be $K_{C_p\_C}$. In this case, $K_{C_p\_B} < K_{C_p\_C}$, if $K_{C_p\_B}$ is used to correct the measured sample specific heat capacity, the result will be lower than the real value.

From the above analysis, error in sample specific heat test can be minimized if $C'_s = C_{s\_calibration}$.

However, the accurate total heat capacity C'_s of the to-be-tested sample is not known before hand so this condition can not be met accurately. But in real TMDSC practice, if the sample's specific heat is known to be in a certain range, at least it is possible to select a sample so that its overall heat capacity is close to that of the calibration sample. For example, at room temperature, many metals have a specific heat close to $3R$ (R=8.314 J/mol K), thus the optimal sample mass should be around $C_{s\_calibration}/3R$. For a 20 mg sapphire calibration sample, we may use a ≅20 mg sample for aluminum based materials or a ≅45 mg sample for copper based ones. Alternatively, the to-be-tested samples with different masses can be tried on the TMDSC to obtain the trend and then a more accurate result can be extrapolated from them, this of course will need more labor work to implement.

Ozawa et al. [10] also used a R/C network model to analyze heat capacity measurement in TMDSC, but no thermal resistance between the thermal couples and the sample/reference was taken into account. Actually, without the extra resistance, the simulated sample heat capacity is much more accurate than can be obtained in a real test.

Hatta [11] proposed a delicate method to eliminate the contact resistance by using the phase angle information. This approach requires that there is no reference material on the reference side but uses the support plate itself as the reference, which is not a typical situation for most users. Besides, according to his model, because the calibration coefficient is a function of modulation frequency, this method requires extensive calibration for each target modulation period with quite a lot of standard samples that cover a wide range of heat capacity values. Although theoretically sound, if the long-term stability of the instrument is not good enough, the calibration process itself could be too overwhelming to be practical. In the same issue, Osaza [12] adopted a similar approach and modified his previous R/C network model on the sample side, the result is also similar thus can be subject to the same limitations.

3.3. Modulation period effect

In both Fig. 6 (simulation) and Fig. 7 (experiment), it is found that shorter modulation period or faster modulation frequency tends to lead to bigger error. Increasing modulation period will make values of specific heat more stable. Besides, simulation results indicated that theoretically, when temperature modulation period approaches infinity, these C_p curves will converge to the real specific heat of the sample material regardless of the sample mass (in a real world situation, the possible downside is that when the modulation period gets too big, slow TMDSC system drift (or system low frequency noise) will get mixed into the deconvoluted temperature signal by Fourier Transform due to the noise/signal frequency spectrum overlapping). Normally, in real practice, modulation periods close to the instrument upper limit are preferred over the lower ones when conducting TMDSC specific heat capacity measurement.

3.4. Modulation amplitude effect

Fig. 9 shows the experimental results of the sapphire disk with a mass of 18.25 mg under different modulation amplitudes, ranging from 0.2 to ca. 8 K.

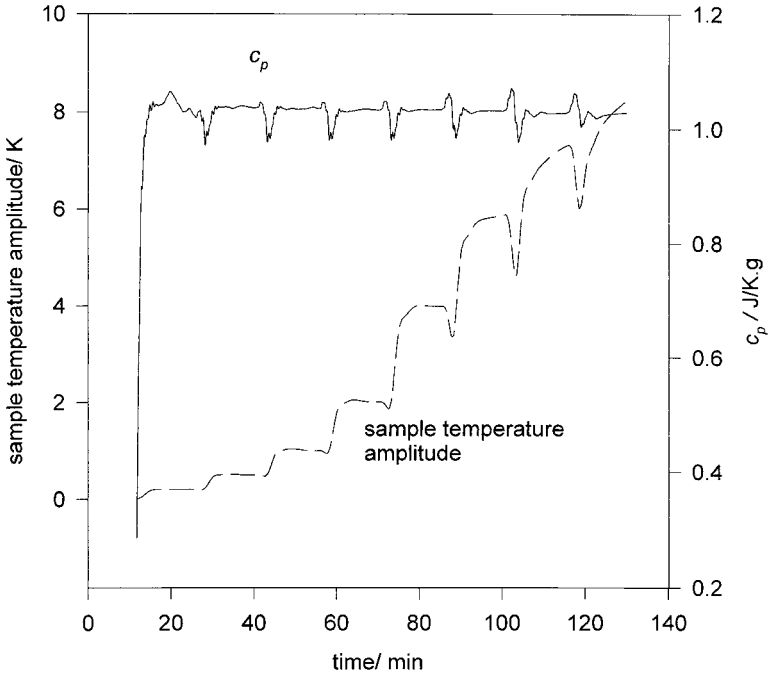

Fig. 9. Effect of temperature modulation amplitude on measured specific heat of sapphire mass: 18.25 mg. Modulation period: 100 s.

Modulation period is fixed at 100 s and isothermal temperature is 400 K. In this figure, the modulation amplitude follows the programmed values closely up to 4 K. When the programmed amplitude is increased further above, the measured temperature amplitude can not quite follow it, yet C_p value varies between 1.027 and 1.034 J/g K among the eight amplitude segments, there is only <1% difference between the maximum and minimum. This figure shows that the modulation amplitude has very little effect on the measured C_p compared with that of the modulation period and sample size. Simulations proved that the temperature modulation amplitude has no effect on the test results at all, which is in good agreement with the experiment.

3.5. Sapphire calibration factor K_{C_p} and mass dependency

Fig. 10 shows the relationship between the calibration factor K_{C_p} and different sapphire disk masses. In this experiment, another standard sapphire disk with a mass of 61.2 mg provided by TA is also used to compare the calibration factors with the previous 18.25 mg sapphire disk. As can be seen here, the 61.2 mg sample exhibits a higher calibration factor than that of the 18.25 mg sample over the whole period range: 10–100 s. For both sapphire samples, K_{C_p} increases with decreasing modulation period. When the period is larger than 60 s, K_{C_p} value becomes relatively stable. Yet, from the curve trend, the K_{C_p} difference between these two sapphire disks will become negligible at a much greater modulation period than the maximum (100 s) available with our current equipment. The implication is, when TMDSC is used to measure materials heat capacities, we not only have to pay attention to the to-be-tested samples, but also have to give some thought to the calibration sample as well, because it will also affect the end results.

3.6. Possible effect of temperature distribution profile inside the sample for metal samples

To evaluate the temperature distribution inside the sample and its possible effect on TMDSC result, simulation was also carried out for this scenery. A cylindrical copper sample with a mass of 200 mg

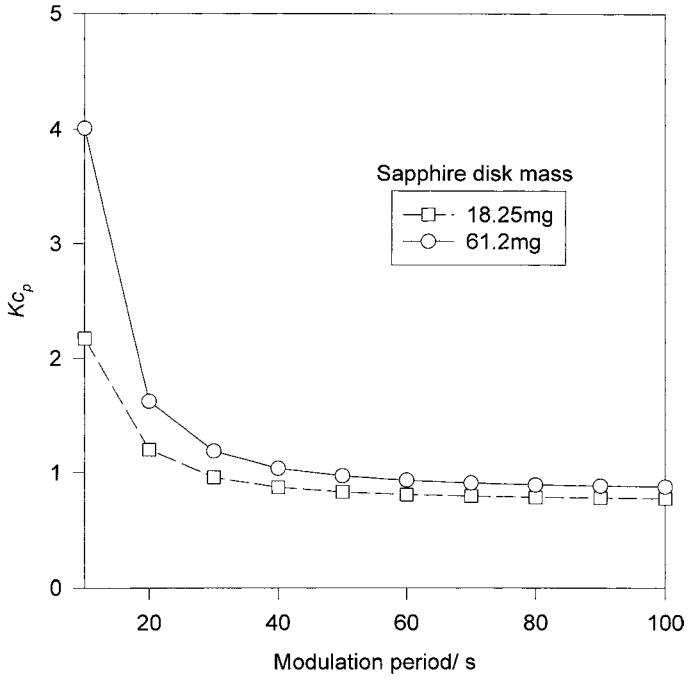

Fig. 10. Calibration factor K_{C_p} mass dependency results of two different sapphire disks.

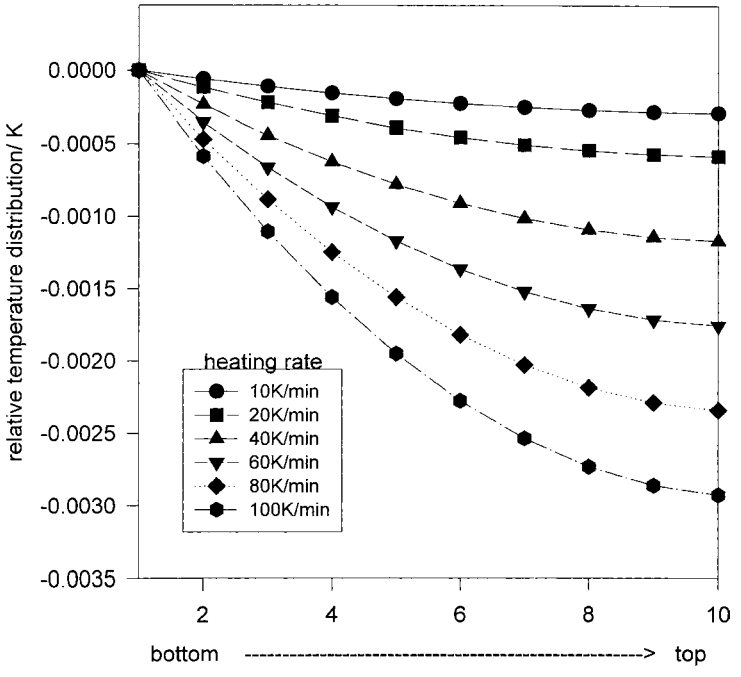

Fig. 11. Relative temperature profile under different linear heating rate inside a 200 mg copper cylinder with a diameter of 6 mm. The bottom temperature is used as a reference point and set as zero. The cylinder is divided into 10 equally sized disks for finite element calculation.

which is much larger than the biggest sample used in our actual experiment and a diameter of 6 mm (this is about the same of the sealing pan's diameter) is assumed to be linearly heated only from the bottom surface. This sample has a thickness of 0.8 mm. By finite element calculation, the relative temperature distribution is given in Fig. 11. Apparently, even under a linear heating rate of 100 K/min, the sample bottom-top temperature difference is only 0.003°C, this is three order's smaller than the typical modulation amplitude. Since the samples used in our experiments are much smaller than 200 mg, besides the maximum instantaneous heating rate in our experiments at a modulation period of 30 s with an 1 K amplitude is 12.6 K/min, which is also much smaller than 100 K/min, for copper and most other metals, the temperature unevenness should not be a major concern in TMDSC tests.

However, for non-conductive materials like polymers, it is worth noting that their heat conducting capabilities is often 2–3 orders lower, in these cases, the thermal resistance of the sample itself can affect the *R*/*C* network profile significantly, the conclusions for metal samples may not apply anymore.

4. Conclusions

In this paper, a *R*/*C* network model is used and solved numerically to analyze the effects of experimental parameters and instrumental thermal properties on specific heat testing in TMDSC under isothermal conditions. TMDSC experiments were conducted with sapphire and pure copper samples correspondingly, with the former to get calibration factors to correct the specific heat of the later. Both simulation and experiments showed that in TMDSC, the measured sample specific heat depends on many factors such as sample size (which was believed to be caused partly by the temperature gradient inside the sample, can also be caused by instrument thermal properties), modulation period, the total heat capacity difference between calibration sample and the to-be-tested samples, etc., but modulation amplitude has very little effect on the test results. The typical behavior of a heat flux type TMDSC instrument can be described by a low pass filter in terms of the relationship between the sample's real specific heat capacity and the measured ones.

Simulation and experiments indicated that when the total heat capacity of the test sample exceeds that of the calibration sample, measured specific heat tends to be lower than its real value, otherwise, it comes higher than the real one.

In TMDSC, at least for metallic materials, where the thermal gradient inside the sample can normally be ignored, with carefully selected test sample size so that its total heat capacity is close to that of the calibration sample and using a long modulation period, more accurate C_p results can be obtained.

References

[1] S.R. Sauerbrunn, B.S. Crow, M. Reading, 21st Proc. NATAS Conf., 13–16 September, Atlanta GA, USA, 1992.
[2] A. Boller, Y. Jin, B. Wunderlich, J. Therm. Anal. 42 (1994) 307.
[3] B. Wunderlich, Y. Jin, A. Boller, Thermochim. Acta 238 (1994) 277.
[4] F.U. Buehler, C.J. Martin, J.C. Seferis, J. Therm. Anal. 54 (1998) 501–519.
[5] F.U. Buehler, J.C. Seferis, Thermochim. Acta 334 (1999) 49–55.
[6] B. Schenker, F. Stager, Thermochim. Acta 304/305 (1997) 219–228.
[7] M. Merzlyakov, C. Schick, Thermochim. Acta. 330 (1999) 65–73.
[8] I.S. Grigoriev, E.Z. Meilikhov, Handbook of Physical Quantities, CRC Press, Inc, 1977.
[9] Operator's Manual, Rev. B. DSC2920 Differential Scanning Calorimetry, TA Instruments, November 1996, pp. C-48.
[10] T. Ozawa, K. Kanari, Thermochim. Acta. 288 (1996) 39–51.
[11] I. Hatta, N. Katayama, J. Therm. Anal. 54 (1998) 577–584.
[12] T. Ozawa, K. Kanari, J. Therm. Anal. 54 (1998) 521–534.